Bioactive Materials 47 (2025) 513–527

Contents lists available at ScienceDirect

Bioactive Materials

journal homepage: www.keaipublishing.com/en/journals/bioactive-materials

A natural biological adhesive from slug mucus for wound repair

Zhengchao Yuan [a,1], Siyuan Wu [b,1], Liwen Fu [c,1], Xinyi Wang [a], Zewen Wang [d], Muhammad Shafiq [e], Hao Feng [a], Lu Han [a], Jiahui Song [a], Mohamed EL-Newehy [f], Meera Moydeen Abdulhameed [f], Yuan Xu [d,**], Xiumei Mo [a,g,*], Shichao Jiang [b,***]

[a] State Key Laboratory for Modification of Chemical Fibers and Polymer Materials, Shanghai Engineering Research Center of Nano-Biomaterials and Regenerative Medicine, College of Biological Science and Medical Engineering, Donghua University, 201620, Shanghai, PR China
[b] Department of Orthopedics, Shandong Provincial Hospital Affiliated to Shandong First Medical University, Jinan, 250021, PR China
[c] Department of Orthopedic Oncology, Shanghai Bone Tumor Institute, Shanghai General Hospital, Shanghai Jiao Tong University School of Medicine, Shanghai, 200080, PR China
[d] Department of Orthopaedics, Xinqiao Hospital, Army Military Medical University, No. 183, Xinqiao Street, Shapingba District, Chongqing, 400037, PR China
[e] Innovation Center of NanoMedicine (iCONM), Kawasaki Institute of Industrial Promotion, Kawasaki-ku, Kawasaki, 210-0821, Japan
[f] Department of Chemistry, College of Science, King Saud University, P.O. Box 2455, Riyadh, 11451, Saudi Arabia
[g] Institute of Biomaterials and Biomedicine, School of Food and Pharmacy, Shanghai Zhongqiao Vocational and Technical University, Shanghai, 201514, PR China

ARTICLE INFO

Keywords:
Wound healing
Tissue regeneration
Slug mucus
Hemostasis
Tissue adhesion

ABSTRACT

Slugs could secrete mucus with multifunctional characteristics, such as reversible gelation, mucoadhesiveness, and viscoelasticity, which can be harnessed for multifaceted biotechnological and healthcare applications. The dried mucus (DM) was prepared using slug, which can be adhered to the tissue surface through different types of interactions (lap-shear force, 1.1 N for DM-3 group). The DM-3 further exhibited the highest hemostatic ability as discerned in a liver trauma injury model (hemostasis time, <15 s), biocompatibility and biodegradability (an insignificant residue at 4 weeks) *in vivo*, and considerably improved skin repair in full-thickness excisional wounds (wound closure, 96.2 % at day 14). Taken together, slug's mucus can be easily prepared with an economic and an eco-friendly method, which may have broad biotechnological and healthcare implications and potential utility in other related disciplines. This transition from natural components to the biomaterial may provide an invaluable platform for different types of applications.

1. Introduction

Acute or chronic wounds due to lacerations, burns, or abrasions, including various ulcers (e.g., venous leg ulcers, diabetic foot ulcer, etc.) pose debilitating health burden worldwide [1,2]. Wound healing primarily aims to promote functional closure, rapid hemostasis, and anti-infection [3]. Traditional dressings, such as cotton gauze and surgical sutures are intensively utilized for wound healing albeit their poor adhesiveness and an additional requirement for the use of foreign objects to fix dressings at wound site [4]. Similarly, while traditional dressings rapidly absorb blood or tissue exudate at injury site, they may cause secondary bleeding and pain during their removal process [5]. Moreover, surgical sutures are commonly utilized for the wound closure, which may induce an additional damage and pain during subsequent removal [6]. Interestingly, the 3M™ (commercial adhesives) could be applied to replace sutures albeit different limitations, including toxicity, incompatibility, and robust adhesion [7].

To address above-mentioned limitations, different types of approaches have been leveraged, including the utilization of natural materials, hydrocolloids, films, foams, hydrogels, and micro/nanofibers [8]. Especially, natural materials play a pivotal role for various biomedical applications, thanks to their easier production,

Peer review under the responsibility of KeAi Communications Co., Ltd.
* Corresponding author. State Key Laboratory for Modification of Chemical Fibers and Polymer Materials, Shanghai Engineering Research Center of Nano-Biomaterials and Regenerative Medicine, College of Biological Science and Medical Engineering, Donghua University, 201620, Shanghai, PR China.
** Corresponding author.
*** Corresponding author.
E-mail addresses: 15123161526@163.com (Y. Xu), xmm@dhu.edu.cn (X. Mo), mailjsc@163.com (S. Jiang).
[1] Z.Y., S. W., and L.F. are co-first authors.

https://doi.org/10.1016/j.bioactmat.2025.01.030
Received 17 October 2024; Received in revised form 29 December 2024; Accepted 22 January 2025

cost-effectiveness, and wider availability [9]. Moreover, natural materials manifest additional characteristics, such as non-toxicity, biocompatibility, biodegradability, and potentially an availability of cell binding motifs [10]. Recently, snail mucus, as a natural product discovered and isolated from snails, has been employed for skin repair [11]. Similarly, slugs' mucus has been shown to exhibit chemical diversity alongside several additional metabolites and an abundance of natural products [12]. The slug mucus can exhibit different types of physical properties (e.g., sticky, clear foamy secretions, etc.), which are mainly ascribed to its versatile content (Fig. 1a). Slug mucus possesses various bioactive components, such as glycoproteins, polysaccharides, peptides, lipids, and secondary metabolites. It is anticipated that these diverse array of natural products may confer multifunctional characteristics to wound dressings, including anti-oxidative ability, anti-microbial ability, anti-inflammatory potential, and tissue repairability (Fig. 1b and c) [12].

Slugs are terrestrial gastropods, which inhabit at a wide range of ecosystems and are composed of a mucus shell layer; the latter leverages an array of functions to the slug, including defense against predation and infection, resistance against slippage for an appropriate locomotion, and moisturization of the host's surface, which may also have potential implications for regenerative medicine and tissue engineering (TE) [13]. Despite these intriguing yet advantageous abilities of the slugs' mucus, including adhesiveness, lubrication, and microbial protection, there is an acute scarcity of the scientific literature of the potential utilization of slug as a biomaterial [14]. Especially, slug's mucus has received only a little attention of the researchers to comprehensively elucidate its structure and function as well as innovatively utilize it for various biotechnological and healthcare related applications [15].

Most of the snails or slugs' mucus can stimulate angiogenesis by binding with various growth factors (GFs), such as vascular endothelial growth factor (VEGF), platelet-derived growth factor (PDGF), and fibroblast growth factor (FGF) [11,16]. Due to oxidative stress, an imbalance occurs between the production of reactive oxygen species (ROS) and cellular antioxidant defense mechanism [17]. Skin repair products contain bioactive components, including glycosaminoglycans (GAGs) from snail's mucus; the latter can impart anti-oxidative and anti-inflammatory effects for various dermatological effects [18]. These salutatory effects are ascribed to snail's mucus-mediated suppression of the gene expression level of the cyclooxygenase-2 (COX-2) [19]. Moreover, slug secretes mucus, which can either inhibit or even kill the bacteria to avoid infection, which is indicative of their significant antibacterial activity [20,21]. Taken together, mucus components could enhance essential cellular processes, while antimicrobial peptides and proteins could be used as novel antimicrobial agents to minimize antibiotic resistance. These advantageous features manifest the potential utilization of the slugs' mucus for different types of healthcare and biomedical applications, such as products for skin repair, aging resistance, inflammation resolution, and microbial resistance, thanks to the diverse array of bioactive compounds alongside structural and functional diversity and tunable physicochemical properties [20,22].

Wound healing encompasses multiple cellular and biological effects. Cells, scaffold, and extracellular matrix (ECM) components work in a concerted manner alongside a spectrum of cytokines, chemokines, and GFs for functional skin tissue repair [16,23]. Thus, wound healing is a dynamic yet a complex process, that involves multiple overlapping phases, such as hemostasis, inflammatory reaction, cell proliferation, and maturation [24]. Thus slug mucus may have considerable potential for skincare and cosmetics products as well as potential utilization as a functional dressing to promote wound healing, thanks to its anti-microbial activitym, anti-inflammatory response, inflammation resolution, [19]. Despite existing positive effects and potential transformation of waste material into valuable resources, the utilization of the natural bioactive components, such as slugs' mucus is still at its infancy for the regenerative medicine and TE applications albeit the dire need of naturally-sourced sustainable bioactive materials for biotechnological, healthcare, and biomedical gains (Fig. 1c). The overarching objective of this research was therefore to sustainably produce slugs' mucus in an environmentally friendly yet a cost-economic manner. Meanwhile, we further elucidate the structure and function of the isolated slugs' mucus using advanced transcriptomics and metabolomics for the potential utilization of slug for practical gains in regenerative medicine and TE, especially for the dermatological applications, including wound healing.

2. Experimental

2.1. Materials

The slugs were purchased from the Qushou Natural Interesting Insect and Plant Museum (Nanyang, China). The NIH-3T3 fibroblasts and human umbilical vein endothelial cells (HUVECs) were obtained from the Typical Culture Collection Committee Cell Bank (Shanghai, China). The P-control dressing (Wound Inorganic Dressing; Dermlin; National Product Approval # 20152140168) was mainly composed of silicon dioxide (SiO_2), calcium carbonate ($CaCO_3$), petroleum jelly and non-woven fabrics and was purchased from Jiangsu Yangsheng Biotechnology Co., Ltd (Jiangyin, China).

2.2. Preparation of dry slug mucus

2.2.1. Collection of mucus

For stable secretion of variouscomponents, slugs were cultured in an homemade insect terrarium at 20 °C and were homogenously reared with lettuce leaves for up to 3 days, and mucus was extracted. Since the mucus is water-soluble, the mucus layer was dissolved in deionized (DI) water by swelling, and solution was collected (Fig. S1). This approach may help extract the mucus while preserving animals' life alongside cost-effectiveness (Fig. 1a). The collected mucus was further diluted and homogenized to obtain a homogenous solution and insoluble foreign matter was removed by centrifugation at 10,000 rotations per minute (rpm) for up to 10 min. To further remove the impurities, the solution was filtered and freeze-dried (Fig. S2).

2.2.2. Preparation of dry slugs mucus

Dry matter content of the collected mucus was very small, which can be rapidly dissolved in an aqueous solution. Consequently, it is imperative to increase the density of the dry mucus to ensure its stability in an aqueous solution. 50 mg, 100 mg, and 200 mg of the dry mucus was dissolved in 10 mL of DI water, poured into a mold, and lyophilized. The lyophilized matter was sterilized with gamma (γ) rays using cobalt (Co)-60 to obtain DM-1, DM-2 and DM-3 scaffolds.

2.3. Analysis of the ingredient in the fresh slug mucus

2.3.1. Proteomic analysis of fresh slugs' mucus

The proteomic analysis of slug mucus was carried out with Hang Zhou KaiTai-Bio CO., LTD (Hang zhou, China) [25]. Briefly, slug mucus was dissolved into lysis buffer solution for protein digestion and labelled with iTRAQ. Liquid Chromatography (LC)-Electrospray Ionization (ESI) Tandem by Q Exactive was used to identify peptides from slug mucus following a previous report [25]. Finally, this information including the peptide mass tolerance, MS/MS tolerance, enzyme, and missed cleavage was used to identify protein.

2.3.2. Untargeted metabolomics analysis of fresh slugs' mucus

Untargeted metabolomics analysis of slugs' mucus was accomplished with Hangzhou KaiTai-Bio CO., LTD (Hangzhou, China) [26]. Briefly, an appropriate amount of slug mucus was added into a 2 mL centrifuge tube containing 400 μL of methanol and was vortexed for 1 min. The mucus was centrifuged at 12,000 rpm for 10 min at 4 °C. The dried sample was redissolved using 150 μL of 2-chloro-l-phenylalanine (concentration, 4

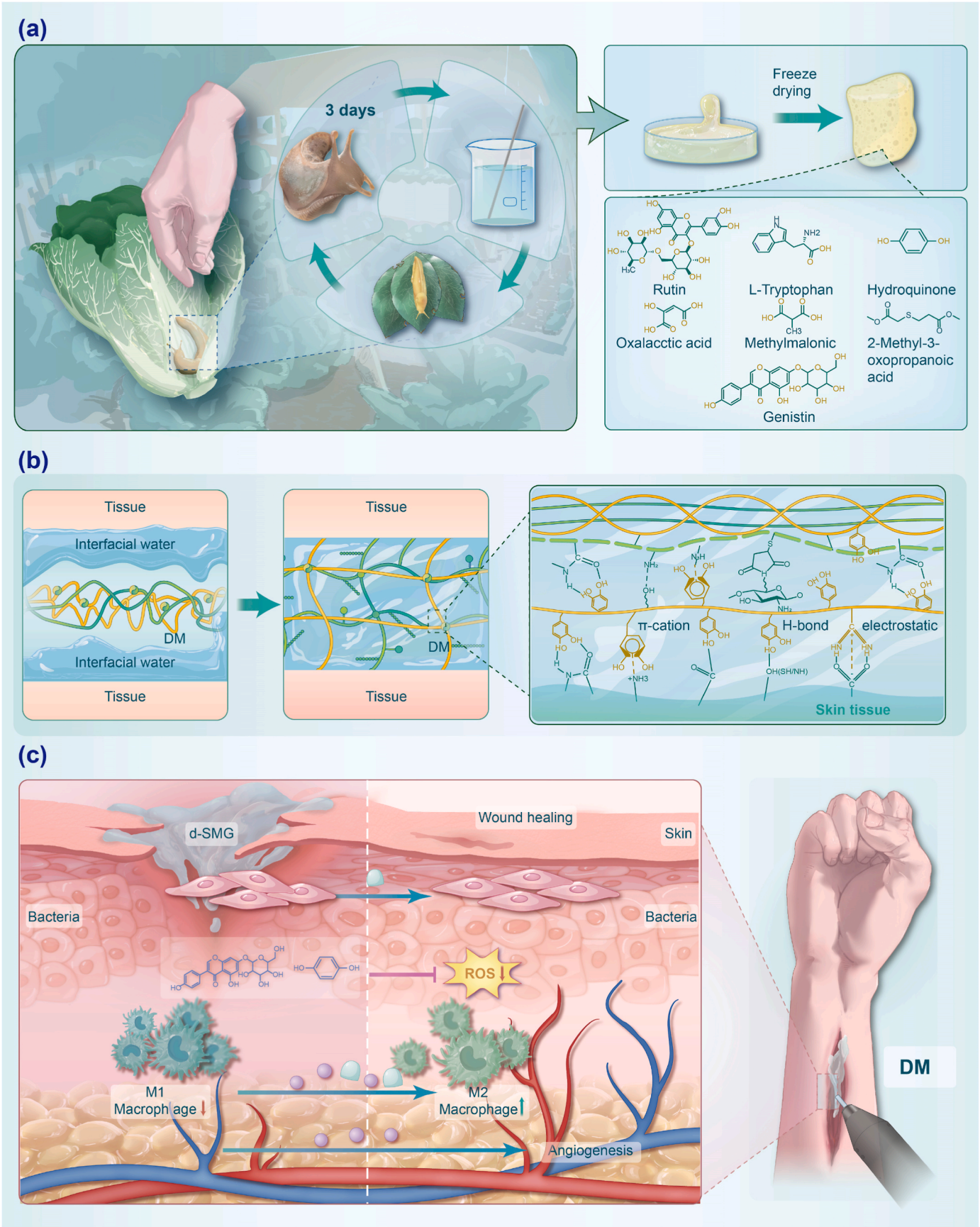

Fig. 1. Schematic illustration of the preparation and wound healing mechanism of DM. (a) Fabrication process and representative structures of small molecules from untargeted metabolomics of DM. (b) The conversion process and mechanism of transition from DM to hydrogel. (c) The postulated mechanism of DM to promote skin tissue repair.

ppm) solution, supernatant was filtered with a 0.22 μm membrane, and transferred into a detection bottle for subsequent analysis by LC-MS. The LC analysis was performed on a Vanquish UHPLC System (Thermo Fisher Scientific, USA), while the chromatography was carried out with an ACQUITY UPLC ® HSS T3 (2.1 × 100 mm, 1.8 μm) (Waters, Milford, MA, USA).

2.4. Network pharmacology analysis

The molecular structural formula of the top 20 untargeted metabolomics components (T20 UMC) was prepared in the section titled *"Untargeted Metabolomics analysis"* and PubChem database. We leveraged top 20 molecular structural formulas alongside keywords, such as "wound healing" to identify target genes according to the literature [27, 28]. The intersection of the potential targets was imported into the Venn diagram, PPI Network Analysis, GO (Gene Ontology) function and KEGG

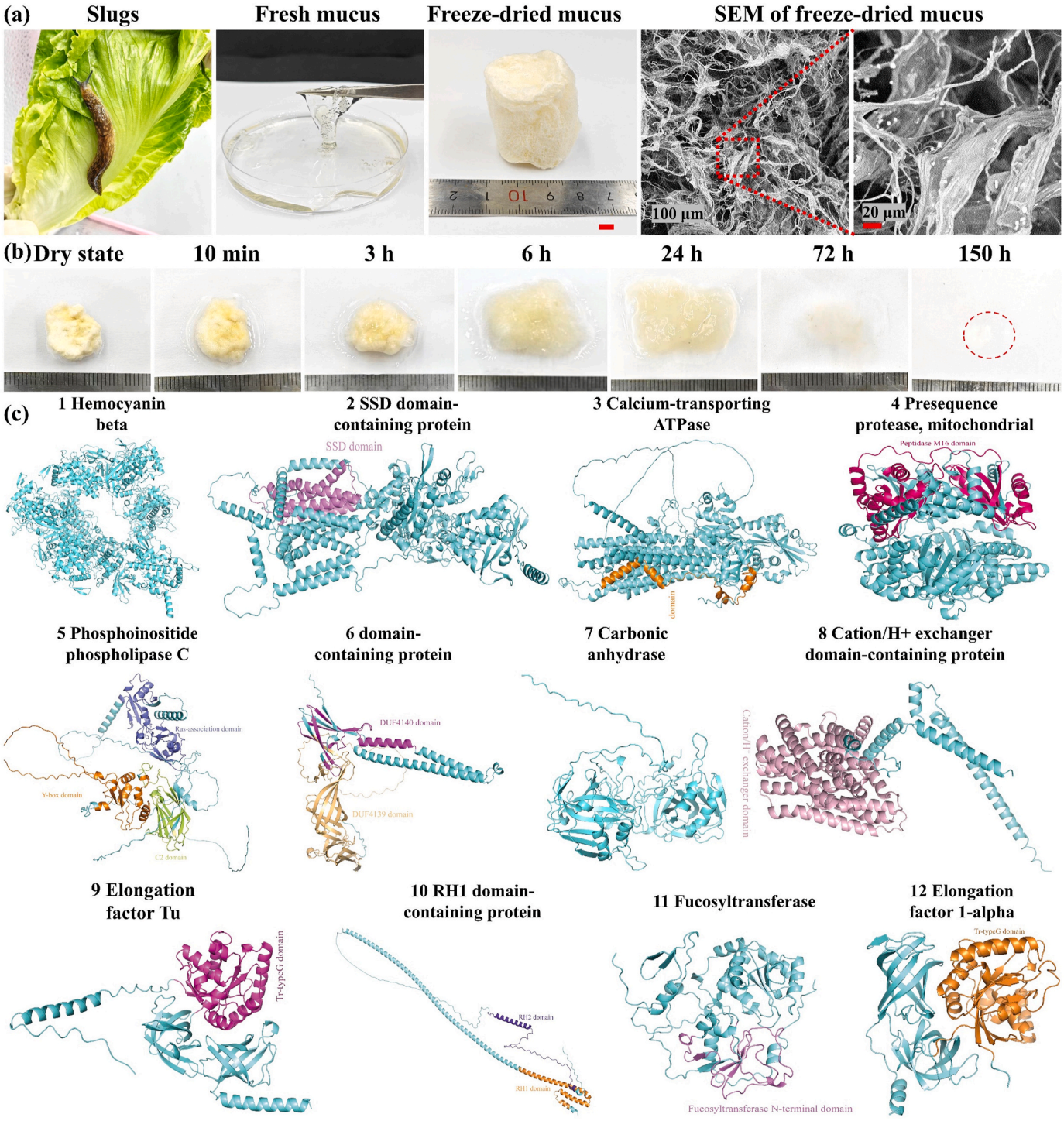

Fig. 2. Characterizations and component assay of slugs mucus. (a) Macroscopic images of slug feeding in the vegetable leaves, fresh slug mucus, freeze-drying mucus, as well as the freeze-drying mucus SEM. (b) The state of DM-3 soaked in the PBS solution at various time points. (c) The top 12 protein structures identified through proteomic analysis.

(Kyoto Encyclopedia of Genes and Genomes) enrichment analysis [29]. The GO enrichment analysis included three modules: cell composition (CC), biological process (BP), and molecular function (MF), and the top 10 modules were selected according to the number of involved targets ($p < 0.05$). Meanwhile, KEGG pathway analysis was selected for the top 30 targets ($p < 0.05$).

2.5. Physico-chemical analysis

The morphology of DM-1, DM-2 and DM-3 was examined by scanning electron microscopy (SEM, Hitachi, TM-1000, Tokyo, Japan). To assay changes after exposure to a liquid on DM-3, the sample was immersed in phosphate-buffered saline (PBS) for up to different time points.

2.6. Biocompatibility and biological functions of scaffolds in vitro

To assay biocompatibility and biological functions of DM scaffolds, a series of *in vitro* tests, including cytocompatibility, transwell, tube formation assay, and blood coagulation index (BCI), were performed. The detailed methods are provided in Supplementary Information.

2.7. Animal experiments

Protocols for animal experiments were approved by the Shandong Provincial Hospital Affiliated with Shandong First Medical University, Shandong, China (Approval # 2024-126). For preliminary biocompatibility assessment, DM-1, DM-2, and DM-3 scaffolds were subcutaneously implanted in Sprague-Dawley (SD) rats for up to 4 weeks. Scaffolds along with adjacent tissues were harvested and subjected to histomorphometric analysis with Hematoxylin and Eosin (H&E) staining and Masson's trichrome (MT) staining. Similarly, the potential of dressings to induce the skin repair was also examined in a full-thickness excisional defect model in SD rats as well as in an anti-scarring ear injury model of rabbits. Detailed methods are provided in Supplementary Information.

3. Results

3.1. Preparation and characterizations of DM

Slugs, as mollusks, could secrete mucus on their body surface to facilitate adhesion to the object surface (Fig. S3). As shown in Fig. 2a, slugs can engulf vegetable leaves and secrete mucus to conformally contact with the surface of various objects by secreting bioactive compounds as they crawl. The mucus exhibits sufficient solubility and therefore can be obtained by soaking an object in DI water (Fig. 2a). The slug-secreted mucus was appeared to be colorless and transparent and was lyophilized into aerogel scaffolds (Fig. 2a). Scaffolds manifested light yellow color after being placed for some period presumably due to the oxidation of the unsaturated components of the dried mucus, thereby implying an anti-oxidative ability of the mucus (Fig. 2a & Fig. S4).

The DM exhibited versatile mucus with different microstructures, and the high mucus displayed strip-like structure with a 3D hollow fibrous structure (Fig. 2a & Fig. S4). The DM-3 could absorb water to form the hydrogels at an initial stage, which can gradually degrade over time (Fig. 2b & Fig. S5). The lap-shear assay was used to discern the tissue adhesive property of DM. The time-force curve manifested that the DM exhibit tissue-adhesion ability (Figs. S6a–b) [30]. The DM-3 exhibited the highest tissue-adhesion ability in all scaffolds, which can be ascribed to the high content of DM with the binding sites to the skin tissue (Figs. S6b–c).

To discern the components of fresh slugs' mucus, proteomic analysis was carried out and specific proteins alongside molecular weight were determined. As shown in Fig. 2c and Tables S1–S3, the slug mucus displayed 52 types of proteins, which were referred to 26 species of well-characterized proteins (e.g., hemocyanin beta, SSD domain-containing protein, calcium-transporting ATPase, resequencing protease and mitochondrial, phosphoinositide phospholipase C, etc.), 13 species of protein fragments (e.g., Tyrosinase copper-binding domain-containing protein, KATNIP domain-containing protein, Kinesin-like protein, U3 small nucleolar RNA-associated protein 25 homologs, etc.), and 13 species of uncharacterized protein. Of these three different protein categories, approximately half of the proteome displayed molecular weight (Mw) more than that of the 50 kDa; several molecules were composed of even Mw more than that of the 200 kDa. These results indicate that the DM is mainly composed of macromolecules with the potential to form the hydrogels (Tables S1–S3).

To further analyze primary metabolites, secondary metabolites, and natural productions, untargeted metabolomics (Mw < 1 kDa) was employed. Fresh slug mucus possessed 31 types of primary metabolites and 42 types of secondary metabolites (Figs. S7 and S8). Primary metabolites included carboxylic acids and derivatives, fatty acyls, organooxygen compounds, pyridines and derivatives, phenols, and indoles and its derivatives (Fig. S7). On the other hand, secondary metabolities included amino acids, peptides and analogs, fatty acids and fatty acid conjugates, carbohydrates and carbohydrate conjugates, pyridine carboxylic acids and their derivatives, and benzenediols (Fig. S8). Moreover, we identified 130 types of natural products, with the high content of betaine, erucic acid, palmitic acid, rutin, 3-hydroxybenzyl alcohol glucoside, nicotinic acid, and hydroquinone. These results indicated the slug's mucus contains the high content of small molecules with the potential anti-oxidative activity (Fig. 3a & Fig. S9).

To delineate biological function of small molecules acting on soft tissue regeneration, the T20 UMC was employed for Network Pharmacology Analysis on "wound healing". T20 UMC displayed 2,122 targets and the wound healing was referred to 5,262 targets, while common targets were 1,004 (Figs. S10a–b). These results indicated that components in the slug's mucus may exhibit the potential to promote wound healing. The correlation of the intersecting targets was further analyzed, which revealed 156 targets with a correlation coefficient more than that of 99.815, including tumor suppressor p53 (TP53), B-cell lymphoma-2 (Bcl-2), albumin (ALB), transforming growth factor-β1 (TGFβ-1), mitogen-activated protein kinase 3 (MAPK3), epidermal growth factor (EGF), interleukin-6 (IL-6), and AKT serine/threonine kinase 1 (AKT-1) (Fig. 3b). These targets mainly involved the resolution of inflammatory response and tissue regeneration.

KEGG enrichment analysis showed that these intersecting targets were mainly referred to the signaling pathways of inflammation regulation and angiogenesis, such as AGE-RAGE (advanced glycation end products-receptor for advanced glycation endproducts) signaling pathway, TNF (tumor necrosis factor) signaling pathway, and PI3K-Akt (phosphatidylinositol 3-kinase-protein kinase B) signaling pathway (Fig. 3c). Moreover, GO enrichment analysis highlighted these biofunctional change in cell proliferation, metabolic activity, and inflammation regulation, including positive regulation of gene expression, positive regulation of cell proliferation, inflammatory response, identical protein binding, protein kinase activity, and protein kinase binding (Fig. 3d–f). Taken together, metabolomics and proteomics results indicate the potential of the slug mucus to promote soft tissue regeneration.

3.2. Biocompatibility and biofunction in vitro

The cytocompatibility of DM was discerned by live/dead staining and CCK-8 assay. The extract solution of the DM manifested good biocompatibility as indicated by enhanced cell vitality and cell spreading at day 5 (Fig. 4a and b & Fig. 4f–g & Fig. S11). The chemotactic effect of DM toward HUVECs and NIH-3T3 fibroblasts was discerned by Transwell migration assay. DM scaffolds, including DM-1, DM-2, and DM-3 recruited significantly more number of cells in comparison to the control group (Fig. 4c and 4h–i). (# of migrated cells, 20.5 ± 3.7, 33.0 ± 4.1, 41.3 ± 5.7, 65.3 ± 6.1 per hpf for NIH-3T3

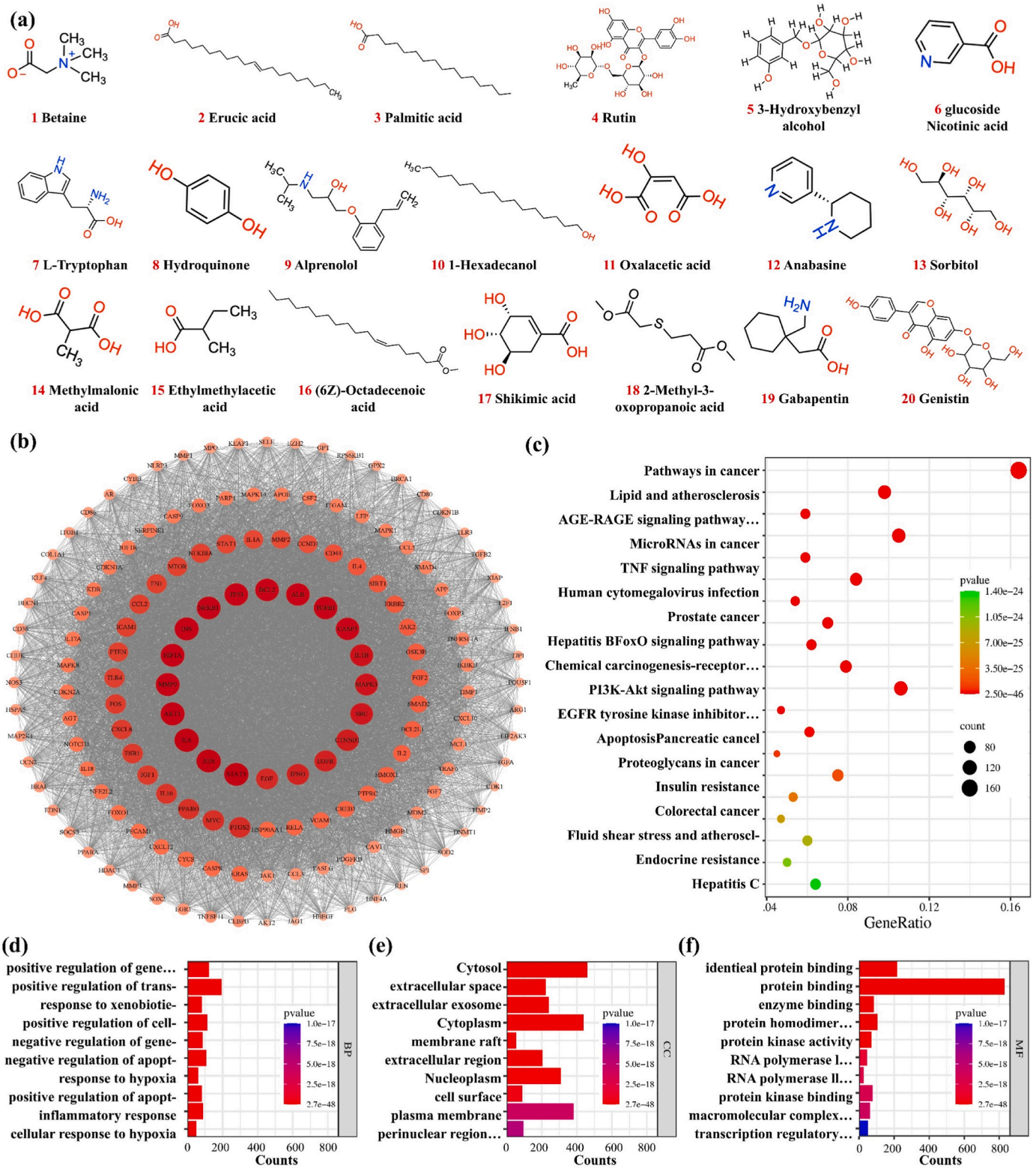

Fig. 3. Network pharmacology analysis. (a) The molecule structure of the top 20 untargeted metabolomics components (T20 UMC). (b) The PPI analysis of core targets of wound healing and T20 UMC. (c) Graph of KEGG enrichment analysis. (d–f) Graph of GO enrichment analysis results.

fibroblasts, and 7.5 ± 3.1, 9.8 ± 3.3, 20.8 ± 4.2, and 32.5 ± 3.9 per hpf for HUVECs in the control, DM-1, DM-2, and DM-3 groups, respectively).

We further discerned angiogenic ability of DM scaffolds using HUVECs *in vitro*. The DM-1, DM-2, and DM-3 groups displayed distinct angiogenic network formation ability in Matrigel *in vitro*. Quantitative analysis showed that the number of meshes were 2.8 ± 1.3, 8.8 ± 3.3, 6.5 ± 1.3, and 5.8 ± 1.0 in the control, DM-1, DM-2, and DM-3 groups, respectively (Fig. 4d & j). These results indicated that DM can facilitate cell growth as well as improve their chemotaxis and tubule-like network formation *in vitro*.

Given the viscous and hygroscopic properties of the DM *in vitro*, coagulation properties were evaluated by the BCI measurement. As

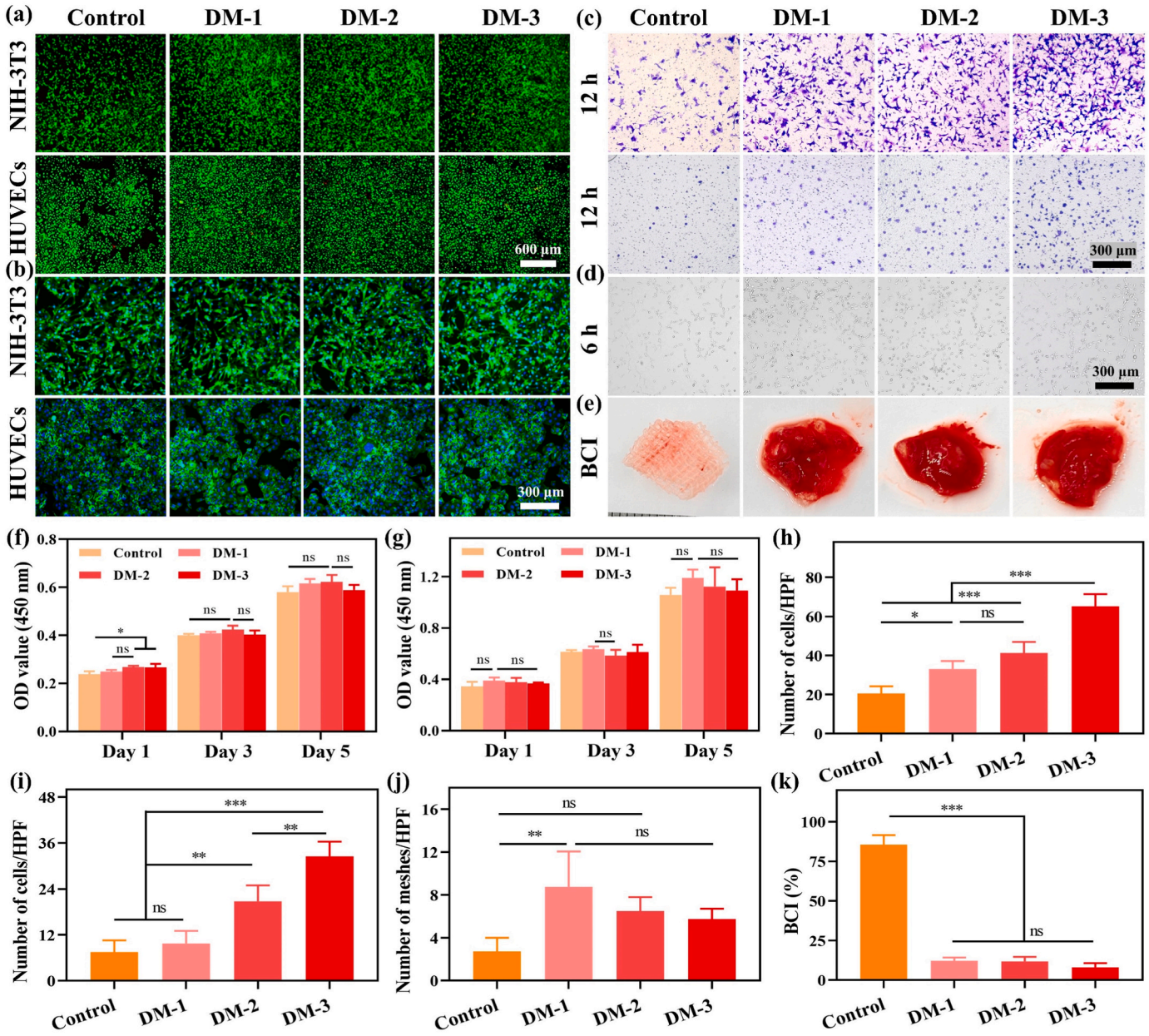

Fig. 4. Biocompatibility and biofunction analysis of scaffolds *in vitro*. (a) Live/dead staining, and (b) DAPI/F-actin staining of NIH-3T3 fibroblasts and HUVECs at day 5. (c) Transwell migration assay of HUVECs and NIH-3T3 fibroblasts at 12 h. (d) Tubule-like network formation of HUVECs at 6 h. (e) Macroscopic images of dynamic whole-blood clotting model of various scaffolds. Quantitative analysis of the proliferation of NIH-3T3 fibroblasts (f), and HUVECs (g) is measured with a CCK-8 assay. Migration ratio of NIH-3T3 fibroblasts (h) and HUVECs (i) in a Transwell assay. The number of meshes (j) and BCI value (k) *in vitro*. *P < 0.05, **P < 0.01, and ***P < 0.001.

shown in Fig. 4k, the BCI value were 85.6 ± 6.0 %, 12.0 ± 2.3 %, 11.7 ± 3.1 %, and 8.0 ± 2.6 % for the control, DM-1, DM-2, and DM-3 groups, respectively. The surface of DM-1, DM-2, and DM-3 groups exhibited distinct blood clots, while the testing solution displayed a light red color due to hemolysis (Fig. 4e). These results indicated the potential of scaffolds to promote coagulation *in vitro*.

3.3. Biocompatibility of scaffolds in vivo

The cytocompatibility and hemocompatibility of the scaffolds *in vitro* indicated the potential of mucus components to improve the biocompatibility. Therefore, we next elucidated the biocompatibility of DM scaffolds *in vivo* for up to 3 weeks (Fig. 5a). As shown in Fig. 5b, DM-1, DM-2, and DM-3 scaffolds displayed the residual scaffold at 1 week, while the lumps of three groups had significantly decreased at 2 weeks post-operatively compared with that of the 1 week. Moreover, DM-1 and DM-2 did not show residual scaffolds 3 weeks post-operatively, while DM-3 still had a small amount of lumpy residue, which can be ascribed to the higher DM content. These results indicated that the DM scaffolds could be degraded *in vivo* (Fig. 5b).

Histological analysis by H&E staining manifested an accumulation of large number of inflammatory cells in all groups, while MT staining showed collagen regeneration as earlier as week 1 post-implantation of scaffolds (Fig. 5c). These results indicated an infiltration of inflammatory cells at an earlier implantation stage of DM scaffolds. H&E staining further revealed significant neo-tissue infiltration, which is indicative of the degradation of scaffolds 3 weeks post-implantation (Fig. 5d). MT staining manifested collagen regeneration in all scaffolds. Scaffolds

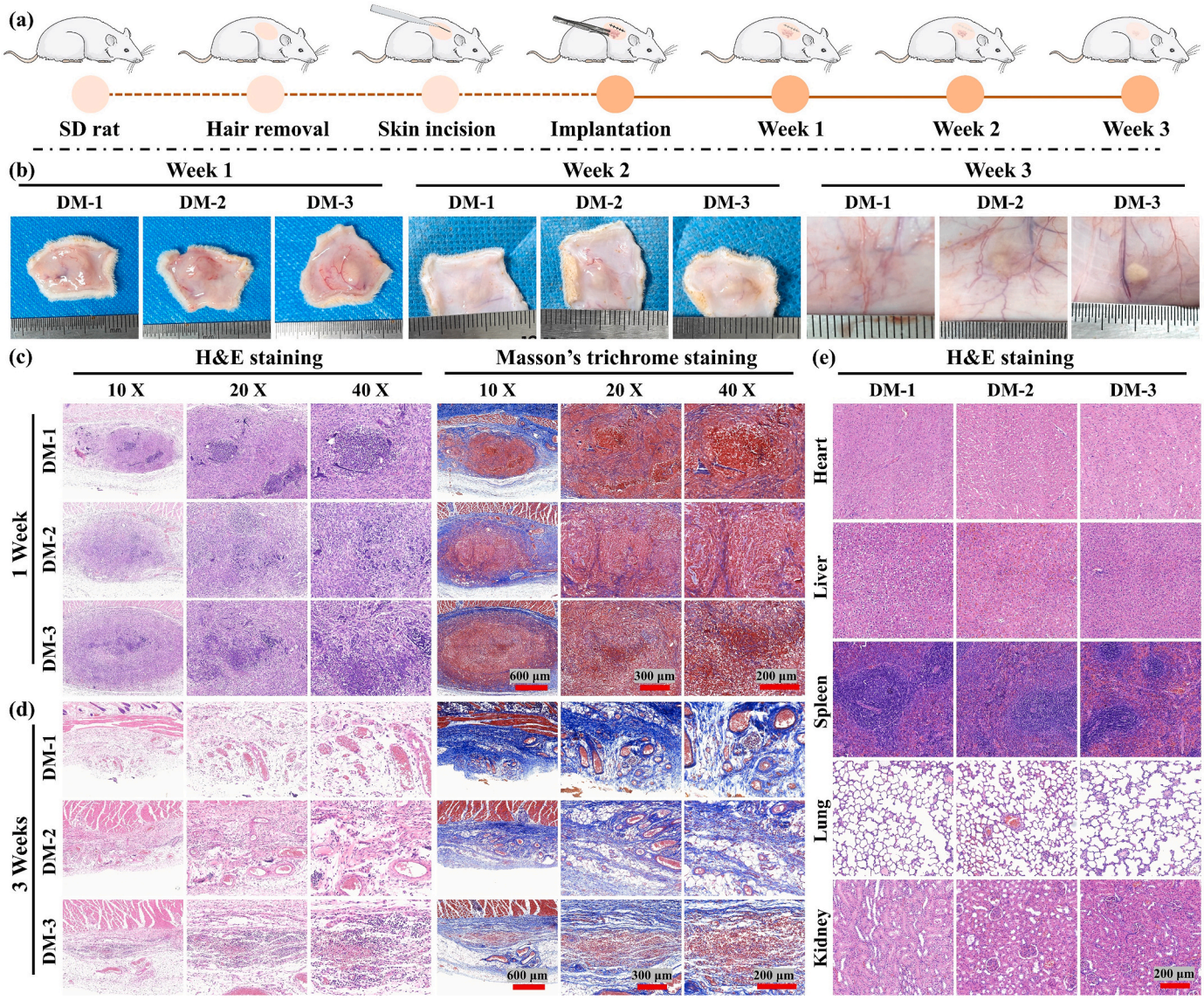

Fig. 5. Biocompatibility of scaffolds *in vivo*. (a) Schematic illustration of the subcutaneous implantation of scaffolds in rats for up to 3 weeks. (b) Photographs showing the samples of subcutaneous implantation at 1, 2, and 3 weeks. H&E staining and MT staining at week 1 (c) and 3 (d) post-implantation. (e) H&E staining of main organs collected from different animals transplanted with DM-1, DM-2, and DM-3 scaffolds at week 3 post-implantation.

containing the low content of the DM-1 were found to be more conducive for the cellular infiltration as well as collagen production presumably owing to their rapid degradation (Fig. 5d). These data revealed potential of scaffolds to promote cellular infiltration, blood vessel formation, and ECM deposition, which may also have implications for the potential of scaffolds for tissue regeneration. H&E staining of main organs, including heart, liver, spleen, lung, and kidney did not manifest the cytotoxicity of the scaffolds (Fig. 5e).

3.4. Adhesion ability of scaffolds in a rat skin incision model in vivo

We next ascertained the potential of DM scaffolds on the tissue adhesion in a skin incision model in SD rats for 4 weeks (Fig. 6a). As shown in Fig. 6b, Bio-adhesives 3M™ as well as DM scaffolds can effectively achieve skin adhesion on both sides of long wounds at day 0. In contrast, wounds did not heal well in the control group, presumably due to the skin tension during the movement. On the other hand, at day 4 and 7 post-operatively, defects in the control groups manifested a reduction in the wound size albeit an incomplete closure. In comparison to the control group, Bio-adhesives 3M™ as well as DM scaffolds were appeared to form scabs at the defect site (Fig. 6b, e-f). DM-2 and DM-3 scaffolds exhibited an inferior wound closure, plausibly due to the presence of the DM at the wound site, which can constrict wound closure owing to its sluggish absorption (Fig. 6b). By day 14, all groups showed almost complete wound closure; the scab layer was found to be peeled away and the neo skin tissues were formed (Fig. 6b).

We observed distinct scar tissue formation in the control and 3M™ groups. Conversely, scar tissue formation was only observed at the suture site in the defects treated with the DM-1, DM-2, and DM-3 groups even at day 28 (Fig. 6b) [6]. While skin incision treated with 3M™ dressings exhibited well-bridged defect healing, residual adhesive was observed at the wound site, which may impair skin repair. Skin regeneration requires re-epithelialization, cellular infiltration, ECM component regeneration, and neovascularization [16]. While H&E staining manifested residual inflammatory cells at the defect site, MT staining showed the deposition of collagen albeit an insignificant difference among different groups (Fig. 6c and d). MT staining further showed more scar length in the 3M™, DM-2, and DM-3 groups in comparison to the other groups, thereby indicating that the residual adhesives may induce scar tissue formation and necessitating further optimization of

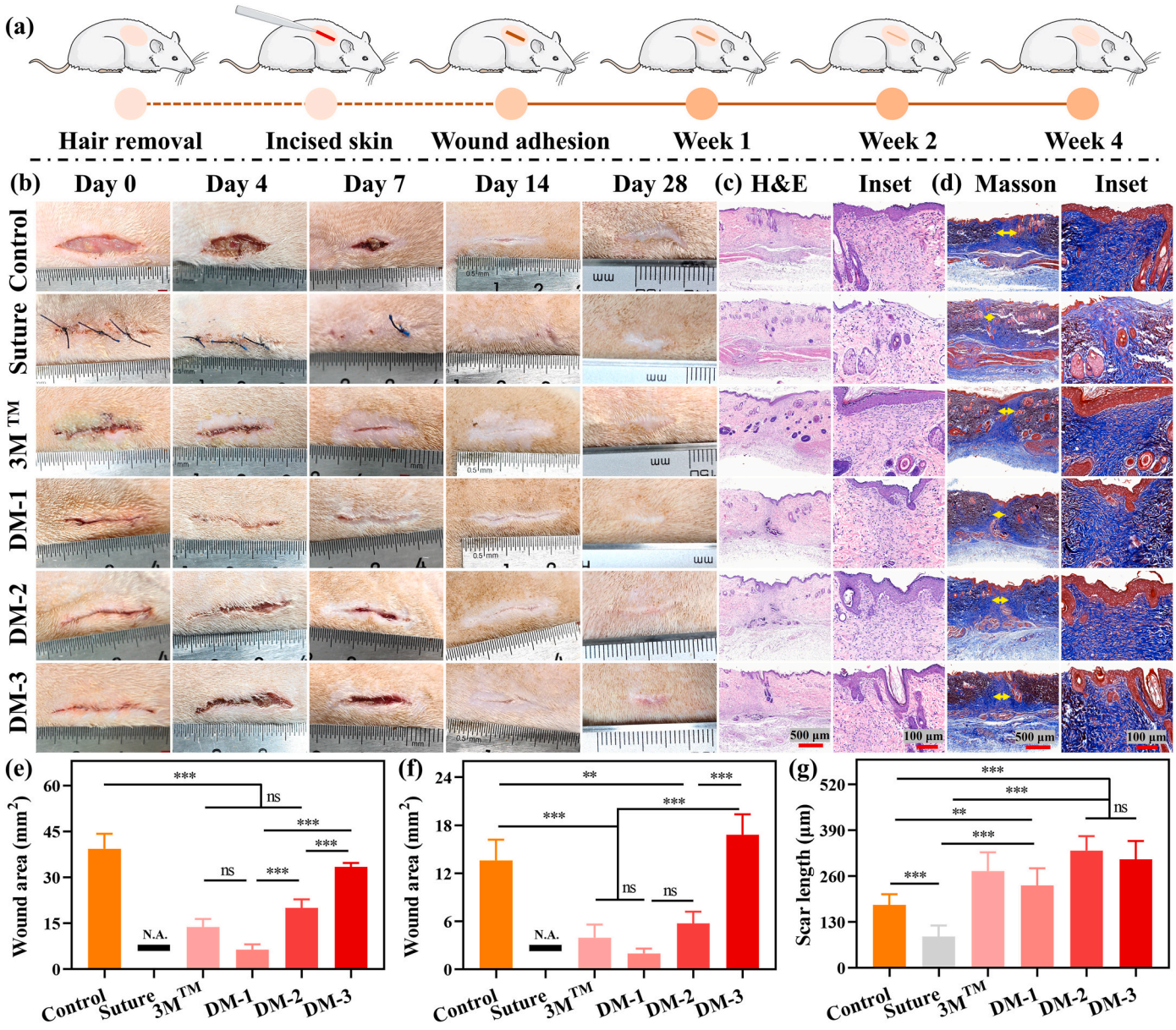

Fig. 6. The wound adhesion efficacy assay *in vivo*. (a) Schematic illustration of the wound adhesion treatment for 4 weeks. (b) Photographs of the rat incised skin after treatments by using various scaffolds for 4 weeks. The H&E (c) and MT (d) staining of the incised skin at 4 weeks. The yellow double-headed arrows indicated the scar. The quantitative analysis of wound area at day 4 (f) and day 7 (g). The scar length analysis at day 28 (h). *P < 0.05, **P < 0.01, and ***P < 0.001.

the composition to induce the wound closure while inhibit the scar tissue formation (Fig. 6d and g).

3.5. Wound healing in vivo

Given the biocompatibility and adhesive properties of the DM, scaffolds were further assessed for the healing of full-thickness excisional defects in rats for up to 2 weeks (Fig. 7a). As shown in Fig. 7b, the wound has a noticeable crust at day 3 in all groups, while the crust was removed at day 7. Both the control group (defects with no treatment) and the P-control group (defects treated with a commercial dressing) exhibited larger residual wounds as compared to their counterparts treated with the DM scaffolds. While wounds in the DM-1 DM-2, and DM-3 groups manifested distinct wound closure at day 10, those in the control and P-control groups exhibited scab on the skin surface (Fig. 7b and e). Taken together the DM scaffolds displayed a superior skin repair ability both in terms of the wound closure and the neo-tissue formation, which may be ascribed to bioactive components of the slugs' mucus and is also in agreement with the findings of the metabolomics and transcriptomics *in vitro*.

The H&E staining showed a large number of residual inflammatory cells at the defect site, while the epithelial layer in the control and P-control groups was thicker compared to normal skin(Fig. 7c, Fig. S12a). The number of inflammatory cells were 26.3 ± 8.5, 38.0 ± 8.6, 21.8 ± 5.5, 18.4 ± 6.6, and 17.9 ± 3.8 per hpf, while the thickness of the epithelial layer was 5.4 ± 1.3 μm, 5.7 ± 1.2 μm, 3.9 ± 0.7 μm, 3.1 ± 0.7 μm, and 3.1 ± 0.6 μm for control, P-Control, DM-1, DM-2, and DM-3 groups, respectively (Fig. 7f and g). Further analysis of the tissue sections for pro-inflammatory, CD68-positive (M1) macrophages and anti-inflammatory, CD206-positove (M2) macrophages revealed significantly more CD206-positive macrophages in DM-1 and DM-3 groups than that of the other groups (Fig. S13). Therefore, wound defects treated with DM-1, DM-2, and DM-3 scaffolds exhibited less number of inflammatory cells and thinner epithelial thickness. The control and P-

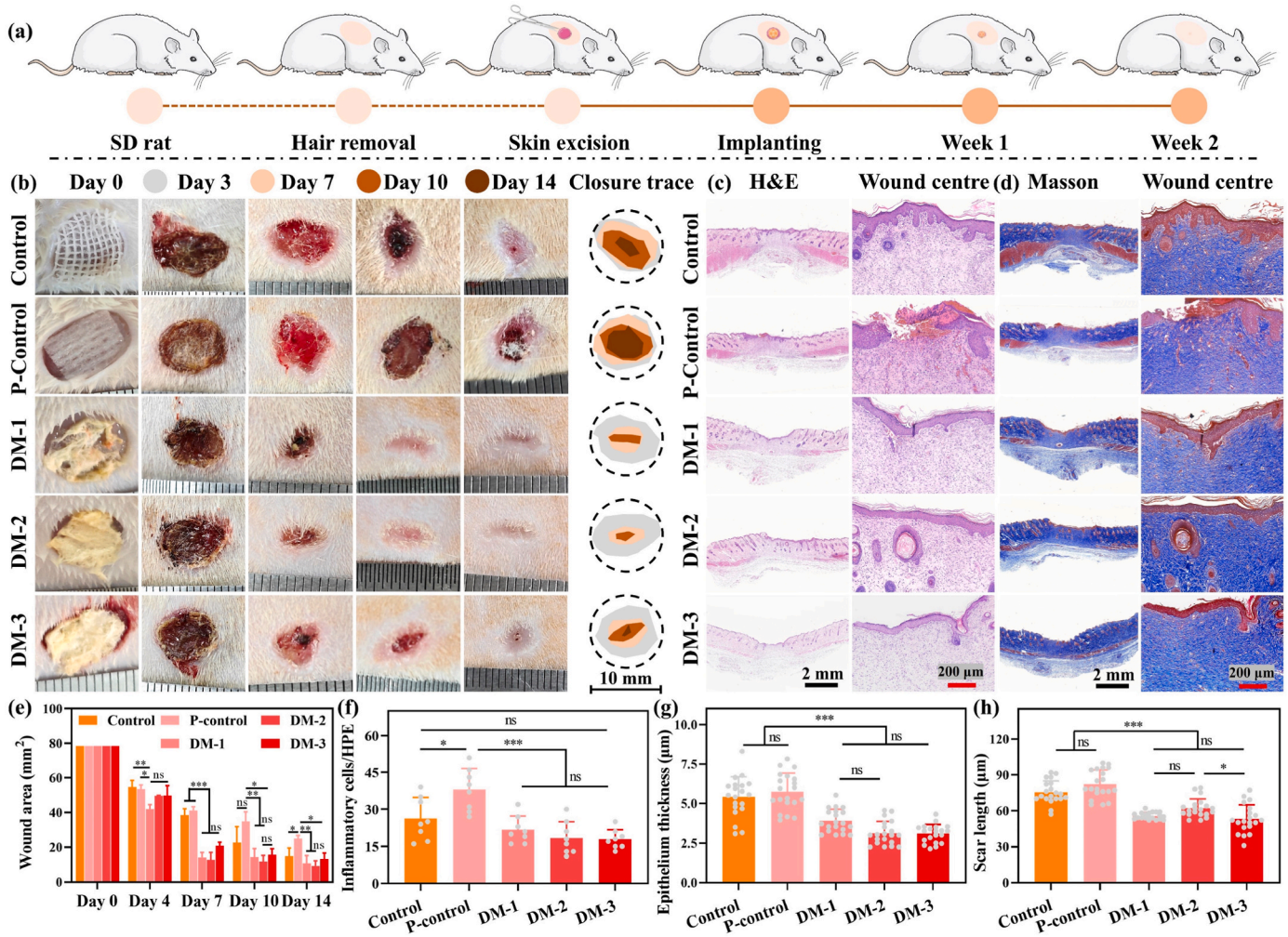

Fig. 7. Evaluation of scaffolds for skin repair in a full-thickness excisional defect model in SD rats. (a) Schematic diagram of the wound treatment for up to 14 days. (b) Representative images of wounds healing by day 14. The H&E staining (c) and MT staining (d) of the wound center and margins at day 14. (e) Wound size at each time point normalized with respect to the day 0. Quantitative analysis of the number of inflammatory cell (f), epithelium thickness (g), and scar length (h) in the wound site at day 14. *P < 0.05, **P < 0.01, and ***P < 0.001.

control groups showed a slower healing ratio and less epithelial thickness than that of the DM-1 and DM-2 groups (Fig. 7d). MT staining displayed an increase in the collagen deposition in all groups over time. DM-1, DM-2, and DM-3 groups displayed significantly higher collagen deposition than the control and P-control groups (Fig. 7d & Fig. S12b). Scar length was respectively 75.4 ± 9.5 μm, 82.2 ± 11.8 μm, 55.7 ± 2.9 μm, 62.1 ± 7.7 μm, and 53.2 ± 11.8 μm in the control, P-Control, DM-1, DM-2, and DM-3 groups, respectively (Fig. 7h). These data showed that the DM scaffolds could effectively mitigate the scar tissue formation.

The whole transcriptome RNA sequencing of regenerated skin was used to discern gene expression level in comparison to the normal skin in the wound microenvironment at day 10 post-operatively. As shown in Fig. 8a, the up- and down-regulated genes in the mucus group were similar to those of the normal group (up-regulated genes, 629 in mucus group v.s. 575 in normal group; down-regulated genes, 1,070 in mucus group v.s. 1,288 in normal group), while the gene expression level of the control group was quite different compared to normal skin, indicating the gene expression of the mucus group was highly similar to that of the normal skin (Fig. 8b–d). The PCA showed remained consistency among the samples within the group, and had obvious differences between the samples (Fig. 8e). Meanwhile, the heatmap of correlation of various groups showed the samples within the group were highly correlated, while the Venn diagram of differential genes for control, mucus, and normal groups displayed the genetic changes among different comparison regimens (Figs. S14a–b).

The GO upregulated enrichment analysis focused on the regulation of cell behavior and tissue regeneration for both mucus and control groups, including cellular component, extracellular region, cell differentiation, cell adhesion, and regulation of gene expression (Fig. 8f). Meanwhile, the GO downregulated enrichment analysis was concentrated on inflammation and immune response for both mucus and control groups, such as inflammatory response, immune response, inflammation resolution, toll-like receptor signaling pathway, and positive regulation of ERK1 and ERK2 cascade (Fig. 8g). The KEGG upregulated enrichment analysis was referred to different transcription factors, MAPK signaling pathway, PPAR (peroxisome proliferator-activated receptors) signaling pathway, FoxO (forkhead box protein O1) signaling pathway, HIF-1 (hypoxia-inducible factor-1) signaling pathway, and Apelin signaling pathway, while the KEGG downregulated enrichment analysis manifested cytokine-cytokine receptor interaction, chemokine signaling pathway, toll-like receptor signaling pathway, Rap1 (Ras-related protein 1) signaling pathway, IL-17 signaling pathway, and TNF signaling pathway (Fig. 8h and i). These results indicated that the mucus can downregulate inflammatory expression, promote cell metabolism and cell viability, and accelerate tissue regeneration.

Wound healing needs to consider not only the wound healing rate, but also the hemostasis performance, and tissue remodeling process

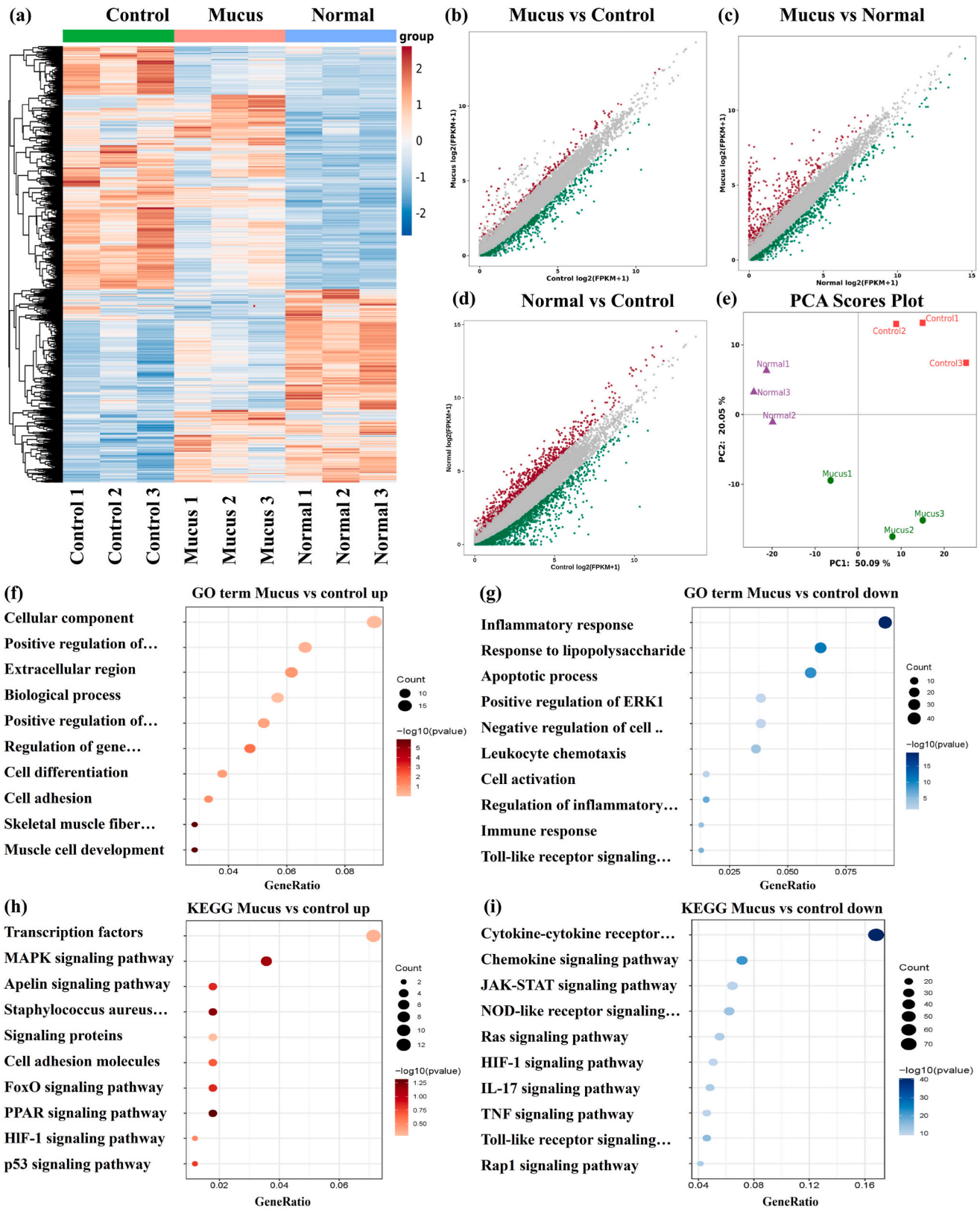

Fig. 8. Whole transcriptome RNA sequencing reveals the wound microenvironment for normal, control, and DM-1 group at 10 days. (a) Heatmap of upregulated and downregulated genes in the wound microenvironment after normal, control, and DM-1 treatment. Volcano plot of the differential gene of Mucus vs Control (b), Mucus vs Normal (c), Normal vs Control (d). Principal component analysis (PCA) of each group (e). The upregulated (f) and downregulated (g) of the top 10 differential genes by GO enrichment analysis between Mucus and Control group. The upregulated (h) and downregulated (i) of the top 10 differential genes by KEGG enrichment analysis between Mucus and the Control group.

after shin repair, such as scar-free tissue regeneration [23]. In comparison to the control group, DM-1, DM-2, and DM-3 groups showed good hemostatic ability, which is ascribed to the rapid uptake of the blood by the DM scaffolds. The DM scaffolds may quickly absorb the blood, transform into a gel-like state, and adhere to the bleeding site, thereby achieving wound hemostasis (Fig. S15). A rabbit ear punch wound model was chosen to discern the ability of the scaffolds to reduce the scar tissue formation during wound healing (Fig. 9a). By day 7, wounds exhibited a scab, which were healed at day 14 post-operatively (Fig. 9d). The wound further underwent tissue remodeling from day 14 for up to day 28. The defects treated with DM-1, DM-2, and DM-3 scaffolds exhibited significantly less injured area than that of the other groups on day 28 (Fig. 9d).

H&E staining exhibited significantly fewer inflammatory cells in DM groups than that of the control and P-control groups (Fig. 9e). The number of inflammatory cells were 25.8 ± 3.8, 126.8 ± 14.5, 111.5 ± 11.4, 96.5 ± 6.6, 86.8 ± 9.5, and 93.0 ± 10.4 per hpf in the normal, control, P-Control, DM-1, DM-2, and DM-3 groups, respectively (Fig. 9b & Fig. S16a). MT staining showed thicker epithelial layer in the control and P-Control groups in comparison to the other groups (Fig. 9e). The thickness of the epithelial layer was 10.1 ± 1.8 μm, 34.2 ± 6.1 μm, 32.7 ± 6.9 μm, 27.5 ± 2.6 μm, 18.7 ± 4.2 μm, and 19.7 ± 2.2 μm in the normal, control, P-Control, DM-1, DM-2, and DM-3 groups, respectively (Fig. 9c and e). Moreover, the MT staining exhibited an obvious collagen regeneration in all groups, while the regenerated collagen in the defects was morphologically similar to the collagen tissues in the normal skin (aligned collagen fibers in the dermal tissue) (Fig. 9e & Fig. S16b). These results indicated the repaired wound of DM treatment has a lighter scar in terms of the epithelial layer thickness and collagen regeneration.

4. Discussion

The utilization of bioactive components holds great promise for the treatment of debilitating diseases, including their potential utilization

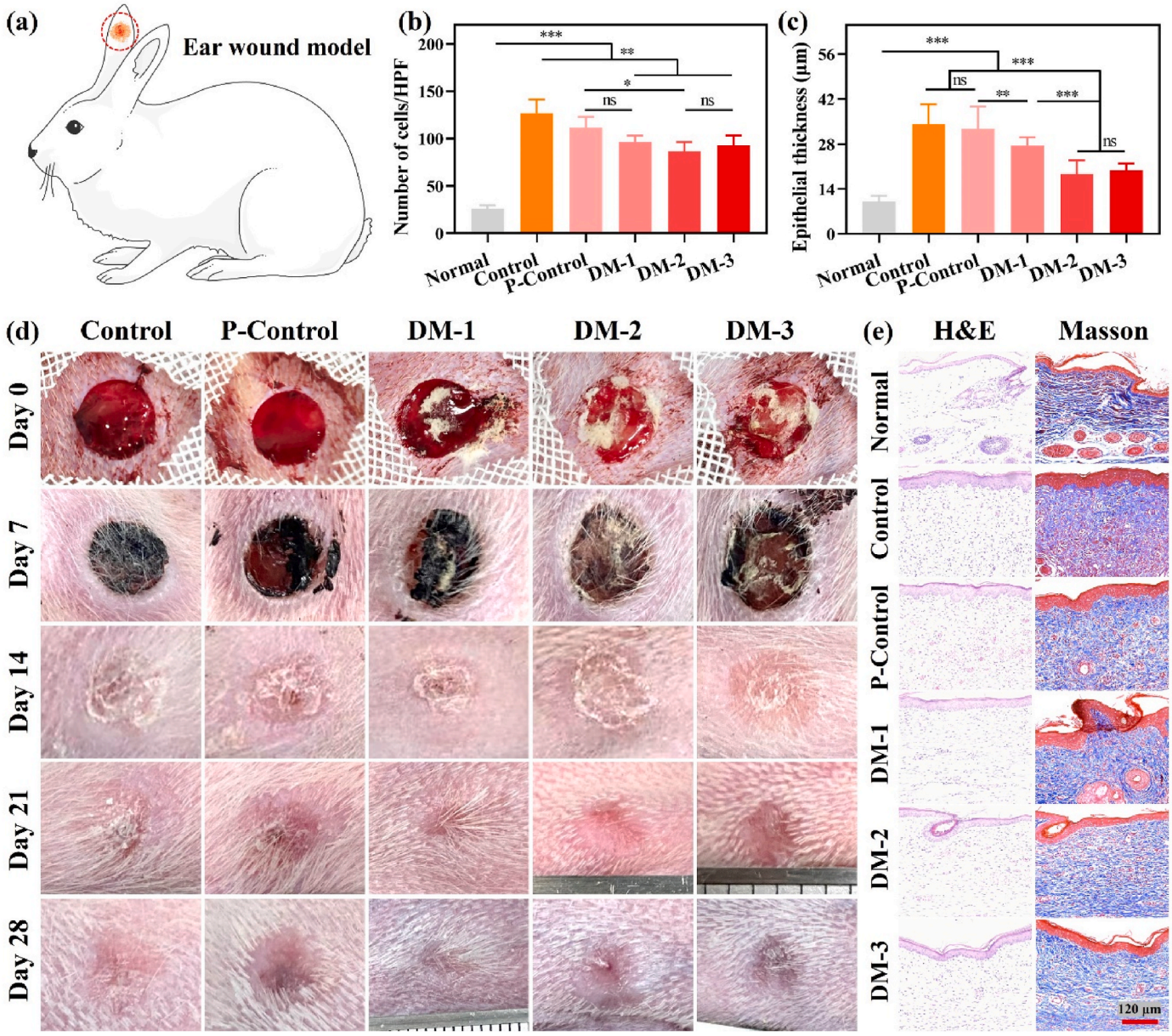

Fig. 9. The wound healing assay in an ear punch wound model in rabbits. (a) Schematic diagram of ear punch wound model. (b) The epithelium tissue thickness, (c) the number of inflammatory cells at the wound site on day 28. (d) Representative images of wound size and scar residue of wounds, as well as (e) the H&E and MT staining for up to 28 days. *P < 0.05, **P < 0.01, and ***P < 0.001.

for regenerative medicine and TE. Herein, we have utilized slugs and obtained the mucus using a gentle and a cost-effective method, which requires the minimal use of animals alongside well-compliance with the animal ethics [31]. Global demand for natural products has substantially increased bioprospecting efforts to obtain novel sources of bioactive ingredients or biomaterials [12]. The majority (>80 %) of pharmaceutical drugs from natural products or natural sources, as well as synthetic products avoid adverse side effects. These natural products have also been exploited for cosmetic applications and skin repair, thanks to an easier availability and cost-effectiveness [19]. Due to these advantages and an increasing utilization of natural materials, the development of biomimetic materials has garnered considerable attention of the research community [6].

Snail mucus has been widely utilized for cosmetics and wound healing applications, and has been shown to promote blood vessel formation and skin repair with minimal side effects [32,33]. These natural medicines exhibit high content of hyaluronic acid (HA), proteoglycans, glycoprotein enzymes, and antibacterial peptides. Taken together, these ingredients of nanomedicine can facilitate wound healing [22,34]. The mucus possesses glycoproteins, such as heavily glycosylated mucins, which constitutes for up to 50−90 % of the mass of the mucus. These glycoproteins can potentially form hydrogels (Fig. 2b) [12]. While smaller peptides and hydrophobic lipids mainly constitute the mucin's network, adhesive functions of the mucus are mainly governed by the mucus' biochemical properties, including lectin content, metal ions, and aromatic amino acids [35]. Moreover, ions, crosslinking networks, and lectin-carbohydrate interactions contribute to physical and chemical properties of mucus as well as its reversible gelation, viscoelasticity, and shape recovery [12]. Consequently, the slug mucus is considered as an attractive material, which can endow multiple functionalities to the healthcare products as well as wound dressings, such as moisturization, microbial protection, and tissue regeneration [11].

The fresh mucus exhibits different types of inorganic metal ions, including copper (Cu), iron (Fe), manganese (Mn), zinc (Zn), which can help gel formation upon the secretion of the mucus [36]. Besides, mucus contains high-molecular-weight organic compounds, such as glycoproteins, enzymes, peptides, as well as protein, glycolic acid, elastin, collagen, allantoin, and other bioactive compounds (Fig. 2c and 3a) [15]. Since mucus is abundant in different types of bioactive compounds, it can serve as a valuable resources for the production of novel formulations with reduced toxicity and minimal side effects for cosmetic- and pharmaceutical-related applications [11].

Nevertheless, fresh slugs' mucus exhibits 91–98 % water, which may not be conducive to regulate the content of active ingredients alongside potential preservation risks [22]. Besides, due to the ability of the slug to adjust its temperature with the habitat environment, the mucus retains for up to 80 % of its original viscosity as temperature is varied from 15 °C to 30 °C. Nonetheless, beyond 45 °C, the viscosity of the mucus decreases for up to 50 % plausibly due to change in protein conformation, which may limit its stable application form [15].

The DM, derived from the fresh mucus, was similar to the sponges alongside adequate gas permeability and moisture/exudate uptake ability, which may also have implications for the absorption of wound exudate and can additionally moisturize the wound microenvironment to potentially facilitate the migration of keratinocytes and the proliferation of fibroblasts at the injury site (Fig. 2b) [37,38]. The DM additionally exhibits significant tissue adhesion ability via multiple interactions (e.g., ionic, covalent, coordination bonds, van der Waals interactions, hydrogen bonding, etc.) [39,40]. Network pharmacology between T20 UMC and wound healing also indicated that DM exhibits an ability to promote soft tissue repair (Fig. 3).

We observed good hemocompatibility and cytocompatibility of DM scaffolds *in vitro* albeit severe inflammatory response at an initial stage of subcutaneous implantation (Fig. 4a and b & Fig. 5b–d). These results indicated that the material was biologically active with the potential to stimulate an inflammatory response of the host [23]. Nevertheless, the inflammatory response was dampened with an increase in the implantation time *in vivo* [41]. Since an aberrant inflammatory response may not be conducive for a healthier tissue repair, further optimizations are required to adjust the composition of slug mucus to modulate the inflammatory response.

Recently, a massive number of patients have been suffering from various skin injuries, which range from minor skin incisions to the severe injuries due to traumatic incidents or chronic wounds [6]. Given the prevalent occurrence of traumatic injuries and persistent chronic wounds, efficient wound management is a major challenge in clinical practice [1]. Now-a-days, surgical sutures and staples, as conventional approaches, are widely used to connect damaged tissues and seal wounds albeit numerous shortcomings, including discomfort, surgical site infection risk, and likelihood of scar tissue formation [42]. While medical adhesives, such as 3M™ can be used to replace sutures, they possess toxicity, incompatibility, and robust adhesion, which necessitate an urgent solution for the alternative adhesives [43]. Surgical sutures may enable wound healing, however, the use of the surgical sutures is limited partly due to their inferior mechanical properties, limited functionality, and potential post-surgical complications [1]. Particularly, mechanical mismatch between rigid dry sutures and soft hydrated tissues may cause inflammation [44]. On the other hand, the braided sutures and rough sutures may cause friction against the contacting tissue, thereby leading to damaged fragile tissues or tissue dissection alongside several other post-surgery complications [45].

Recently, natural tissue adhesives, including snail mucus have been used to overcome some of the above-mentioned limitations alongside several other merits, such as cost-effectiveness, non-invasive, and pain relief [2,46]. Meanwhile, the natural adhesion with underlying molecular and biological mechanisms offers a promising platform to promote tissue regeneration [47,48]. The DM possessed bio-integration and healing in the pathophysiological conditions and prevented dressing detachment from the target tissue due to their strong tissue adhesion. The DM displayed good biocompatibility and coagulation properties *in vitro* (Fig. 4a and e). Meanwhile, subcutaneous implantation assay showed that the DM could facilitate host's cell infiltration and enhance the deposition of ECM components andblood vessel formation, which may have implications for their applications *in vivo* (Fig. 5c and d).

It has been further reported that the snail's mucus can facilitate wound repair by enhancing the proliferation of fibroblasts alongside the positive regulation of cell cycle, Col-I secretion, and the regulation of actin cytoskeleton and metalloproteinase (MMP) activity [19]. The whole transcriptome RNA sequencing revealed that the DM could downregulate inflammatory environment, promote cell viability and metabolism, and accelerate tissue regeneration (Fig. 8). In the meantime, the snail's mucus has been shown to possess anti-inflammatory characteristics alongside the potential to improve blood vessel regeneration and play a pivotal role during the remodeling phases of wound healing [12]. We also observed significant wound healing potential of DM in this study, and observed significant wound adhesion efficacy and the healing of the full-thickness excisional defects *in vivo* (Fig. 6b & 7b) [30].

Interestingly, the DM could from gel-like cushion similar to the protective skin barrier to avoid wound desiccation, and mechanical damage (Fig. 2b). The lectins and glycoproteins of the DM could additionally facilitate the trapping and clearance of microbes from outside invasion. Meanwhile, the gel-like state of the DM could provide a moist environment at the injury site, which may help avoid scar tissue formation during wound healing (Fig. 9d) [49]. The DM could also trigger the formation of barrier membrane by the rapid absorption of the wound exudate at the bleeding site, platelet aggregation, and the conversion of the fibrinogen into fibrin, thereby effectively promoting the hemostasis (Fig. S14) [8].

For wound healing, different types of scaffolds are used, such as granular hydrogels, fibrous membranes, hydrogels, and aerogels and other application forms [41]. These scaffolds are usually fabricated

using an array of natural and synthetic polymers alongside crosslinkers and complex fabrication methods [2]. The nanofiber dressings such as poly(lactic-co-glycolic acid)/gelatin (PLGA/Gel) exhibit good permeability and drug delivery efficacy [5]. Nevertheless, long degradation cycle and relatively poor hydrophilicity of artificial synthetic polymers may limit their application prospects in clinical settings [23]. On the other hand, hydrogel dressings, including carboxymethyl chitosan/dextran may enable a moist wound environment albeit various risks, such as weak mechanical properties, uncontrolled degradation, and limited biological activity [50].

Meanwhile, these conventional scaffolds often require complex device handling, cross-linking to improve stability, and the incorporation of additional bioactive components to endow the dressings with the biological functionalities, which in turn prolong the cycle time as well as the production cost [51]. DM scaffold displayed aerogel-like characteristics, which can be transformed into a hydrogel with certain adhesion ability upon exposure with water, which could provide a conducive microenvironment of soft tissue regeneration [8]. DM scaffolds possess large content of bioactive components, which may avoid additional modification or further processing to incorporate biological functionalities to the dressings (Fig. 3b–f). Therefore, DM scaffolds may offer several distinct advantages over conventional dressings.

This study also has several limitations. While DM further exhibited antimicrobial protection, which can be ascribed to the different types of bioactive components, such as lectins, enzymes, and cationic peptides, while their relative functions are unknown. Meanwhile, slugs could secrete various different types of mucus in response to different stimuli or different food, which may lead to the mucus with varying structures and compositions. Moreover, DM belong to microorganism-derived product, which needs to be further subjected to long-term immunological evaluation and in-depth toxicological analysis for the tissue engineering applications. Especially, to fully realize the potential and application of mucus, key challenges of sustainable production, variability, stable storage and rigorous translation through preclinical and clinical testing must be addressed.

5. Conclusion

In summary, the DM from slugs' secretion is a renewable and a sustainable resource and contains a spectrum of bioactive components, which displayed tissue adhesion, hemostatic effect, good biocompatibility and hemocompatibility *in vitro*, as well as biocompatibility, biodegradability, and pro-healing activity for wound healing *in vivo*. These advancements provide opportunities to achieve an efficient wound healing strategy and improve patient outcomes, which may offer a promising solution for multifaceted biomedicine applications.

Ethics approval and consent to participate

Protocols for animal experiments were approved by the Shandong Provincial Hospital Affiliated with Shandong First Medical University, Shandong, China (Approval # 2024-126).

CRediT authorship contribution statement

Zhengchao Yuan: Writing – original draft, Software, Funding acquisition, Data curation, Conceptualization. **Siyuan Wu:** Resources, Formal analysis, Data curation. **Liwen Fu:** Validation, Resources, Formal analysis. **Xinyi Wang:** Visualization, Resources, Formal analysis. **Zewen Wang:** Validation, Methodology, Formal analysis. **Muhammad Shafiq:** Software, Methodology, Data curation. **Hao Feng:** Visualization, Formal analysis, Data curation. **Lu Han:** Validation, Data curation. **Jiahui Song:** Software, Data curation. **Mohamed EL-Newehy:** Validation, Software, Funding acquisition. **Meera Moydeen Abdulhameed:** Validation, Funding acquisition. **Yuan Xu:** Writing – review & editing, Supervision, Funding acquisition. **Xiumei Mo:** Writing – review & editing, Supervision, Project administration, Funding acquisition, Conceptualization. **Shichao Jiang:** Writing – review & editing, Supervision, Funding acquisition, Conceptualization.

Declaration of competing interest

The authors declare that they have no known competing financial interests or personal relationships that could have appeared to influence the work reported in this paper.

Acknowledgments

This research was supported by Taishan Scholars Program of Shandong Province (tsqn201812141), Shandong Provincial Natural Science Foundation (ZR2021MH004), Science and Technology Commission of Shanghai Municipality, China (No. 20DZ2254900) and Sino German Science Foundation Research Exchange Center, China (M – 0263), China Education Association for International Exchange (2022181). This project was also supported by Researchers Supporting Project Number (RSP2025R65), King Saud University, Riyadh, Saudi Arabia, the Science and Technology Research Program of Chongqing Municipal Education Commission (Grant No. KJZD-K202412807) Youth Doctoral Talent Incubation Program of the Second Affiliated Hospital, Army Medical University (2023YQB002). This project was also supported by China Postdoctoral Science Foundation (2023M742325) and the Fundamental Research Funds for the Central Universities and Graduate Student Innovation Fund of Donghua University (CUSF-DH-D-2024040). Thanks for http://www.home-for-researchers.com for creating Fig. 1.

Appendix A. Supplementary data

Supplementary data to this article can be found online at https://doi.org/10.1016/j.bioactmat.2025.01.030.

References

[1] X. Ma, Q. Bian, J. Hu, J. Gao, Stem from nature: bioinspired adhesive formulations for wound healing, J. Contr. Release 345 (2022) 292–305.
[2] Z. Yuan, Y. Zhao, M. Shafiq, J. Song, J. Hou, Y. Liang, X. Yu, Multi - functional fibrous dressings for burn injury treatment with pain and swelling relief and scarless wound healing, Adv. Fiber. Mater. 5 (2023) 1963–1985.
[3] J. Zhu, Y. Li, W. Xie, L. Yang, R. Li, Y. Wang, Q. Wan, X. Pei, J. Chen, J. Wang, Low-swelling adhesive hydrogel with rapid hemostasis and potent anti-inflammatory capability for full-thickness oral mucosal defect repair, ACS Appl. Mater. Interfaces 14 (48) (2022) 53575–53592.
[4] Y. Mao, M. Chen, R. Guidoin, Y. Li, F. Wang, G. Brochu, Z. Zhang, L. Wang, Potential of a facile sandwiched electrospun scaffold loaded with ibuprofen as an anti-adhesion barrier, Mater. Sci. Eng. C. 118 (2021) 111451.
[5] Z. Yuan, M. Shafiq, H. Zheng, L. Zhang, Z. Wang, X. Yu, J. Song, B. Sun, M. El-newehy, H. El-hamshary, Multi-functional fibrous dressings for infectious injury treatment with anti-adhesion wound healing, Mater. Des. 235 (2023) 112459.
[6] T. Deng, D. Gao, X. Song, Z. Zhou, L. Zhou, M. Tao, Z. Jiang, L. Yang, L. Luo, A. Zhou, L. Hu, H. Qin, M. Wu, A natural biological adhesive from snail mucus for wound repair, Nat. Commun. 14 (2023) 396.
[7] R. Stone, E.C. Saathoff, D.A. Larson, J.T. Wall, N.A. Wienandt, S. Magnusson, H. Kjartansson, S. Natesan, R.J. Christy, Accelerated wound closure of deep partial thickness burns with acellular fish skin graft, Int. J. Mol. Sci. 22 (2021) 1590.
[8] Z. Yuan, L. Zhang, M. Shafiq, X. Wang, P. Cai, A. Hafeez, Y. Ding, Z. Wang, M. El-newehy, M. Moydeen, L. Jiang, X. Mo, Y. Xu, Composite superplastic aerogel scaffolds containing dopamine and bioactive glass-based fibers for skin and bone tissue regeneration, J. Colloid Interface Sci. 673 (2024) 411–425.
[9] K. Techawongstien, T. Lirdwitayaprasit, S. Pairohakul, Mucus from the pulmonate sea slug onchidium typhae: biochemical composition and ecological implications for the intertidal community, Mar, Ecol. 43 (2022) e12702.
[10] S.P. Malliappan, A.A. Yetisgin, S.B. Sahin, E. Demir, S. Cetinel, Bone tissue engineering: anionic polysaccharides as promising scaffolds, Carbohydr. Polym. 283 (2022) 119142.
[11] A.A. El-attar, H.B. El-wakil, A.H. Hassanin, B.A. Bakr, T.M. Almutairi, M. Hagar, B. H. Elwakil, Z.A. Olama, Silver/snail mucous PVA nanofibers: electrospun synthesis and antibacterial and wound healing activities, Membranes 12 (2022) 536.
[12] M. Liegertová, J. Malý, Gastropod mucus: interdisciplinary perspectives on biological activities, applications, and strategic priorities, ACS Biomater. Sci. Eng. 9 (10) (2023) 5567–5579.

[13] R. Takano, E. Hirose, Optical properties of body mucus secreted from the coral reef sea slugs: measurement of refractive indices and relative absorption spectra, Zool. Stud. 63 (2024) e2.
[14] Q. Peng, X. Gong, R. Jiang, N. Yang, R. Chen, B. Dai, R. Wang, Performance and characterization of snail adhesive mucus as a bioflocculant against toxic microcystis, Ecotoxicol. Environ. Saf. 270 (2024) 115921.
[15] E. Barajas-Ledesma, C. Holland, Probing the compositional and rheological properties of gastropod locomotive mucus, Front. Soft Matter 3 (2023) 1201511.
[16] Y.B. Rosanto, C.Y. Hasan, R. Rahardjo, T.W. Pangestiningsih, Effect of snail mucus on angiogenesis during wound healing, F1000Research 10 (2021) 181.
[17] J. Li, J. Ma, H. Sun, M. Yu, H. Wang, Q. Meng, Z. Li, D. Liu, J. Bai, G. Liu, X. Xing, F. Han, B. Li, Transformation of Arginine into Zero-Dimensional Nanomaterial Endows the Material with Antibacterial and, Osteoinductive Activity 9 (2023) eadf8645.
[18] S. Been, J. Choi, H. Cho, G. Jeon, J.E. Song, A. Bucciarelli, G. Khang, Preparation and characterization of a soluble eggshell membrane/agarose composite scaffold with possible applications in cartilage regeneration, J. Tissue Eng. Regen. Med. 15 (2021) 375–387.
[19] M. Rashad, S. Sampò, A. Cataldi, S. Zara, Biological activities of gastropods secretions: snail and slug slime, Nat. Products Bioprospect. 13 (2023) 42.
[20] E. Wargala, A. Zalewska, M. Sławska, I. Kot, Snail mucus as an innovative ingredient used in the cosmetology and medical industry, Aesthetic Cosmetol, Med 12 (2023) 45–49.
[21] M.F. Di Filippo, S. Panzavolta, B. Albertini, F. Bonvicini, G.A. Gentilomi, R. Orlacchio, N. Passerini, A. Bigi, L.S. Dolci, Functional properties of chitosan films modified by snail mucus extract, Int. J. Biol. Macromol. 143 (2020) 126–135.
[22] E. Waluga-Kozłowska, K. Jasik, D. Wcisło-Dziadecka, P.O.L. Przemysław, K. Kuźnik-Trocha, K. Komosińska-Vassev, K. Olczyk, M. Waluga, P. Olczyk, A. Zimmermann, Snail mucus - a natural origin substance with potential use in medicine, Acta Pol, Pharm.-Drug Res. 78 (2021) 793–800.
[23] Z. Yuan, L. Zhang, S. Jiang, M. Shafiq, Y. Cai, Y. Chen, J. Song, X. Yu, H. Ijima, Y. Xu, X. Mo, Anti-inflammatory, antibacterial, and antioxidative bioactive glass-based nanofibrous dressing enables scarless wound healing, Smart Mater. Med. 4 (2023) 407–426.
[24] Z. Ahmadian, A. Correia, M. Hasany, P. Figueiredo, F. Dobakhti, M.R. Eskandari, S. H. Hosseini, R. Abiri, S. Khorshid, J. Hirvonen, H.A. Santos, M.A. Shahbazi, A hydrogen-bonded extracellular matrix-mimicking bactericidal hydrogel with radical scavenging and hemostatic function for pH-responsive wound healing acceleration, Adv. Healthc. Mater. 10 (2021) 2001122.
[25] Y. Zhu, H. Xu, H. Chen, J. Xie, M. Shi, B. Shen, X. Deng, C. Liu, X. Zhan, C. Peng, Proteomic analysis of solid pseudopapillary tumor of the pancreas reveals dysfunction of the endoplasmic reticulum protein processing pathway, Mol. Cell. Proteomics 13 (2014) 2593–2603.
[26] S. Abdelrazig, L. Safo, G.A. Rance, M.W. Fay, E. Theodosiou, P.D. Topham, D. H. Kim, A. Fernández-Castané, Metabolic characterisation of Magnetospirillum gryphiswaldenseMSR-1 using LC-MS-based metabolite profiling, RSC Adv. 10 (2020) 32548–32560.
[27] S. Cong, Y. Feng, H. Tang, Network pharmacology and molecular docking to explore the potential mechanism of urolithin A in combined allergic rhinitis and asthma syndrome, Naunyn-Schmiedeberg's Arch. Pharmacol. 396 (2023) 2165–2177.
[28] G. Cao, J. Liu, H. Liu, X. Chen, N. Yu, X. Li, F. Xu, Integration of network pharmacology and molecular docking to analyse the mechanism of action of oregano essential oil in the treatment of bovine mastitis, Vet. Sci. 10 (2023) 350.
[29] W. Deng, W. Zhang, Q. He, Study on the mechanism of puerarin against osteoarthritis from ferroptosis based on network pharmacology and bioinformatics, Naunyn-Schmiedeberg's Arch. Pharmacol. 397 (2024) 959–968.
[30] M. Huang, Z. Yuan, G. Fu, J. Dong, Y. Sun, W. Wang, M. Shafiq, H. Cao, X. Mo, J. Chen, An injectable antibacterial wet-adhesive for meniscal cartilage regeneration via immune homeostasis mediated by SMSC-derived extracellular vesicles, Compos. Part B Eng. 291 (2025) 111970.
[31] M. Itoh, K. Nakayama, R. Noguchi, K. Kamohara, K. Furukawa, K. Uchihashi, S. Toda, J.I. Oyama, K. Node, S. Morita, Scaffold-free tubular tissues created by a bio-3D printer undergo remodeling and endothelialization when implanted in rat aortae, PLoS One 10 (2015) e0145971.
[32] J. Wang, Y. Cheng, L. Chen, T. Zhu, K. Ye, C. Jia, H. Wang, M. Zhu, C. Fan, X. Mo, In vitro and in vivo studies of electroactive reduced graphene oxide-modified nanofiber scaffolds for peripheral nerve regeneration, Acta Biomater. 84 (2019) 98–113.
[33] Y. Shi, P. Rupa, B. Jiang, Y. Mine, Hydrolysate from eggshell membrane ameliorates intestinal inflammation in mice, Int. J. Mol. Sci. 15 (2014) 22728–22742.
[34] G.H. Farjah, B. Heshmatian, M. Karimipour, A. Saberi, Using eggshell membrane as nerve guide channels in peripheral nerve regeneration, Iran, J. Basic Med. Sci. 16 (2013) 901–905.
[35] P.Y. Hayashida, P.I. da Silva Júnior, Limacus flavus yellow slug: bioactive molecules in the mucus, BioRxiv. https://doi.org/10.1101/2021.05.06.442857.
[36] J. Gould, J.W. Valdez, Terrestrial slug uses a vertical bridge of mucus to descend rapidly from heights, Austral Ecol. 46 (2021) 680–682.
[37] Y. Dong, Y. Zheng, K. Zhang, Y. Yao, L. Wang, X. Li, J. Yu, B. Ding, Electrospun nanofibrous materials for wound healing, Adv. Fiber Mater. 2 (2020) 212–227.
[38] T. Mehrabi, A.S. Mesgar, Z. Mohammadi, Bioactive glasses: a promising therapeutic ion release strategy for enhancing wound healing, ACS Biomater. Sci. Eng. 6 (10) (2020) 5399–5430.
[39] J. Li, X. Yu, E.E. Martinez, J. Zhu, T. Wang, S. Shi, S.R. Shin, S. Hassan, C. Guo, Emerging biopolymer-based bioadhesives, Macromol. Biosci. 22 (2022) 1–18.
[40] S. Singh, A. Gupta, D. Sharma, B. Gupta, Dextran based herbal nanobiocomposite membranes for scar free wound healing, Int. J. Biol. Macromol. 113 (2018) 227–239.
[41] Z. Yuan, S. Wu, L. Fu, M. Shafiq, Y. Liang, P. Li, X. Wang, H. Feng, R. Hashim, S. Lou, M. El-newehy, M. Moydeen, W. Zhang, X. Mo, S. Jiang, Composite scaffolds based on egg membrane and eggshell-derived inorganic particles promote soft and hard tissue repair, Compos. Part B. 292 (2025) 112071.
[42] Y. Li, S. Liu, J. Zhang, Y. Wang, H. Lu, Y. Zhang, G. Song, F. Niu, Y. Shen, A. C. Midgley, W. Li, D. Kong, M. Zhu, Elastic porous microspheres/extracellular matrix hydrogel injectable composites releasing dual bio-factors enable tissue regeneration, Nat. Commun. 15 (2024) 1377.
[43] S. Pal, J. Shin, K. DeFrates, M. Arslan, K. Dale, H. Chen, D. Ramirez, P. B. Messersmith, Recyclable surgical, consumer, and industrial adhesives of poly (α-lipoic acid), Science. 385 (2024) 877–883.
[44] A. Sensini, C. Gotti, J. Belcari, A. Zucchelli, M.L. Focarete, C. Gualandi, I. Todaro, A.P. Kao, G. Tozzi, L. Cristofolini, Morphologically bioinspired hierarchical nylon 6,6 electrospun assembly recreating the structure and performance of tendons and ligaments, Med. Eng. Phys. 71 (2019) 79–90.
[45] D. Lin, M. Li, L. Wang, J. Cheng, Y. Yang, H. Wang, J. Ye, Y. Liu, Multifunctional hydrogel based on silk fibroin promotes tissue repair and regeneration, Adv. Funct. Mater. 34 (2024) 2405255.
[46] M.A. Cutuli, A. Guarnieri, L. Pietrangelo, I. Magnifico, N. Venditti, L. Recchia, K. Mangano, F. Nicoletti, R. Di Marco, G.P. Petronio, Potential mucosal irritation discrimination of surface disinfectants employed against SARS-CoV-2 by *Limacus flavus* slug mucosal irritation assay, Biomedicines 9 (2021) 424.
[47] A.M. Smith, P. Huynh, S. Griffin, M. Baughn, P. Monka, Strong, Non-specific adhesion using C-lectin heterotrimers in a molluscan defensive secretion, Integr. Comp. Biol. 61 (2021) 1440–1449.
[48] J. Melrose, High performance marine and terrestrial bioadhesives and the biomedical applications, Molecules 27 (2022) 8982.
[49] L. Chen, Y. Guo, L. Chen, K. Hu, L. Ruan, P. Li, X. Cai, B. Li, Q. Shou, G. Jiang, Injectable Zn^{2+} and paeoniflorin release hydrogel for promoting wound healing, ACS Appl. Bio Mater. 6 (6) (2023) 2184–2195.
[50] H. Byun, Y. Han, E. Kim, I. Jun, J. Lee, H. Jeong, S.J. Huh, J. Joo, S.R. Shin, H. Shin, Cell-homing and immunomodulatory composite hydrogels for effective wound healing with neovascularization, Bioact. Mater. 36 (2024) 185–202.
[51] X. Han, S. Chen, Z. Cai, Y. Zhu, W. Yi, M. Guan, B. Liao, Y. Zhang, J. Shen, W. Cui, D. Bai, A diagnostic and therapeutic hydrogel to promote vascularization via blood sugar reduction for wound healing, Adv. Funct. Mater. 14 (2023) 221308.